

# Consideration of NDVI and Surface Temperature Calculation from Satellite Imagery in Urban Areas: A Case Study for Gumi, Korea

Bhang, Kon Joon<sup>1)</sup> · Lee, Jin-Duk<sup>2)</sup>

## Abstract

NDVI (Normalized Difference Vegetation Index) plays an important role in surface land cover classification and LST (Land Surface Temperature Extraction). Its characteristics do not fully carry the information of the surface cover typically in urban areas even though it is widely used in analyses in urban areas as well as in vegetation. However, abnormal NDVI values are frequently found in urban areas. We, therefore, examined NDVI values on whether NDVI is appropriate for LST and whether there are considerations in NDVI analysis typically in urban areas because NDVI is strongly related to the surface emissivity calculation. For the study, we observed the influence of the surface settings (i.e., geometric shape and color) on NDVI values in urban area and transition features between three land cover types, vegetation, urban materials, and water. Interestingly, there were many abnormal NDVI values systematically derived by the surface settings and they might influence on NDVI and eventually LST. Also, there were distinguishable transitions based on the mixture of three surface materials. A transition scenario was described that there are three transition types of mixture (urban material-vegetation, urban material-water, and vegetation-water) based on the relationship of NDVI and LST even though they are widely distributed.

Keywords: Geometric Shape, Color, Surface Setting, Transition, NDVI, LST

## 1. Introduction

The term, 'urban' can be defined as "a place-based characteristic that incorporates elements of population density, social and economic organization, and the transformation of the natural environment into a built environment" (Weeks, 2010). It was incorporated with many in-situ datasets to observe changes of vegetation and urban areas. NDVI (Normalized Difference Vegetation Index) that typically comes with the remote sensing technology and investigations over green vegetation areas have been a breakthrough in terms of change detection over urbanization as well as vegetation because it takes several advantages of describing land surface conditions like greenness evaluation, surface

material emissivity calculation, relative urbanization to vegetation, etc. in urban areas.

The identification of the urban covers with the remote sensing imagery often causes great confusion because the spectral reflectance of urban materials are sensitive to the characteristics and conditions of the cover materials in pixels of an image such as spectral mixture, aging, and texture of different urban materials. Therefore, urban covers are too complex to be characterized with remote sensing images. Such limitation can be partially coped with various types of indices measuring specific surface cover features, for example, vegetation, water or urban covers. For vegetation, there are more than 150 VIs appeared in scientific articles but a small subset has proved to be useful after systematic

---

Received 2017. 01. 25, Revised 2017. 02. 09, Accepted 2017. 02. 27

1) Member, Dept. of Civil Engineering, Kumoh National Institute of Technology (E-mail: [bhang.l@kumoh.ac.kr](mailto:bhang.l@kumoh.ac.kr))

2) Corresponding Author, Member, Dept. of Civil Engineering, Kumoh National Institute of Technology (E-mail: [jdlee@kumoh.ac.kr](mailto:jdlee@kumoh.ac.kr))

This is an Open Access article distributed under the terms of the Creative Commons Attribution Non-Commercial License (<http://creativecommons.org/licenses/by-nc/3.0>) which permits unrestricted non-commercial use, distribution, and reproduction in any medium, provided the original work is properly cited.

tests. Stagakis *et al.* (2010) grouped VIs into several categories depending on how they are calculated and what properties should be detected. They can be divided into two categories depending on the data source; broadband greenness (appropriate with broadband multispectral sensors to measure the overall amount of vegetation) and narrowband greenness (appropriate with narrowband hyperspectral sensors for more advanced measures of general quantity of green vegetation than the broadband one).

One of the important findings with vegetation index is that areas with less vegetation have higher LST than those with more vegetation. (Carlson *et al.*, 1994; Gillies and Caroson, 1995; Owen *et al.*, 1998; Price, 1990; Gallo *et al.*, 1993; Gallo *et al.*, 1995; Southworth, 2004; Yue *et al.*, 2007). This relationship established a connection between NDVI and LST so that they are inversely proportional with complex interactions of surface materials. An important finding from the NDVI-LST relationship is that the emissivities of land surface materials can be estimated with NDVI values, eventually resulting in the radiant temperatures of materials in urban or vegetation areas (Valor and Caselles, 1996; Jiménez-Muñoz *et al.*, 2008). NDVI, however, has not provided enough information due to seasonal variations of NDVI (Yuan and Bauer, 2007). The complexity of a mixture of land cover materials has a high possibility to propagate errors in the LST extraction from satellite TIR (Thermal Infrared) images typically in urban areas.

NDVI values are influenced by the complexity of various spectral mixtures of materials in a pixel such as shadow, road, building, vegetation, soil, etc. (Wu and Murray, 2003). This provides users to carefully use NDVI because NDVI was developed for the detection of the chlorophyll in vegetation and they often include errors by artificial colors and shadow in vegetation, urban, soil and water pixels. It is not recommended using NDVI for the analysis in the urban. NDVI, however, often plays a pivotal role in LST calculation typically with Landsat TIR images because, for example, the NDVI threshold method (Sobrino *et al.*, 2004) provides the most essential information on emissivity of land surface materials at the exact time of the TIR image capture of Landsat. Here, users fall into a dilemma that they are using the method for emissivity even though NDVI might include

errors in urban areas.

Unfortunately, the cause of spectral characteristics affecting NDVI values have been rarely studied typically in urban areas. Therefore, we attempted to investigate how the NDVI and temperature values of urban cover materials change with the settings of surface materials, for example, colors and shapes of the surface materials and to understand how NDVI and LST behaves with surface material settings. The settings were segmented by simplifying the urban cover types as buildings, asphalt, soil (or bare ground), vegetation and water including the shapes of rooftops and colors for buildings. Based on this, we described a scenario how NDVI changes with mixture of the materials relative to the LST in the Gumi area where man-made structures were widely spread so that man-made materials such as rooftop and asphalt could be easily delineated with Landsat images.

## 2. Datasets and Data Processing

### 2.1 Datasets

We used three different datasets, Landsat 5 TM images, digital topographic maps, and aerial photographs. Landsat 5 TM images were used to calculate NDVI and LST with two different dates on June 15, 2009 and June 22, 2010. High resolution aerial photographs on Oct. 2010 were used as ground truth. Unfortunately, there were time differences between the Landsat images and the aerial photographs, so the aerial photos were minimally used to identify the cover materials. The digital topographic map by the National Geographic Information Institute (NGII) of Korea in November 2010 is a dataset including detailed land use/cover and geographic feature information. It has very comprehensive thematic layers with more than a hundred natural and man-made features, such as transportation, water system, open water, various man-made structures (i.e., buildings and facilities, historic products of civilization, classified vegetation, feature boundaries, topographic information, etc.). All of these features are grouped with three levels in the map; for example, the first level has 8 large categories divided into 104 subcategories at the third level. The digital map was obtained on the web (<http://www.nsic.go.kr/ndsi/main.do>) in the map scales of 1:5,000. The format

is DXF and can be easily converted to shapefiles of ArcGIS with the NGIMap software developed by NGII. This dataset is the best digital map that have ever been made in terms of accuracy and usability specifically for Korea. The digital map coordinate system, Transverse Mercator on GRS80 with the Eastern Origin (false easting = 200,000 m and false northing = 600,000 m), were firstly transformed to WGS84 UTM Zone 52N of Landsat. Since ArcGIS does not have the definition file of the TM coordinate system with the specialized origins like eastern, middle, and western origins of TM for Korea, NGIMap is the most convenient tool to transform between the coordinate systems.

Fig. 1 shows the data processing scheme with atmospheric correction, classification, masking, and calculation of various component to retrieve NDVI and LST.

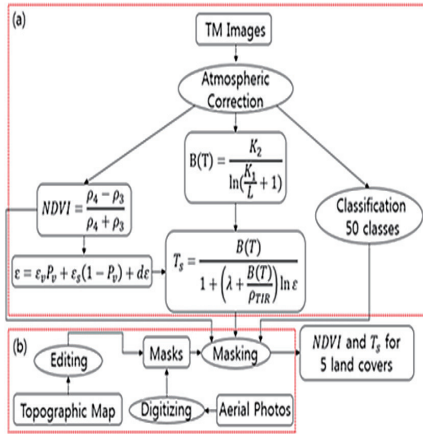


Fig. 1. Schematic data processing diagram

## 2.2 Atmospheric correction for Landsat 5 TM images

The energy from the sun through the earth is dissipated due to various molecules or particles in the atmosphere, thus spectral reflectance for each TM band should be corrected using actual or modeling atmospheric data. Correction methods using the data might not clearly remove the atmospheric effect because of the uncertainties in the atmospheric condition. However, we believe that application of the correction is better than the raw images so we followed the typical correction method. For the atmospheric

correction, MODTRAN codes generated the atmospheric parameters for the two specific data and they were applied to correct the images.

## 2.3 Calculation of NDVI and LST

The atmospherically corrected images of red and near-IR bands were used to calculate NDVI as shown in Fig. 1. Calculation of LST is much more complex than NDVI because LST requires emissivity values for each pixel of the images. The difficulty in calculating emissivity and brightness temperature is that they always comes together in Eq. (1). To solve the equation, one of them must be fixed. In other words, the equation cannot be solved with the single Landsat thermal IR band.

$$\epsilon = \frac{M_e}{M_e^0} \quad (1)$$

where  $M_e^0 = \sigma T^4$  and  $M_e = \epsilon \sigma T^4$ .

We adopted an alternative method by Sobrino *et al.* (2004) to calculate LST values for the given NIR images. The Eq. (2) requires NDVI values for bare soil and full vegetation to calculate the  $P_v$  value. Selecting the NDVI value for full vegetation was made by visual inspection, in which vegetation pixels covered the dense forest area excluding the soil and urban covers. Bare soil was rather difficult to be selected so the value for bare soil was chosen using masking the bare soil area. Based on this methods, we selected the average NDVI value of 0.1 for bare soil and NDVI = 0.8 for pure vegetation.

$$\epsilon = \epsilon_v P_v + \epsilon_s (1 - P_v) + d\epsilon \quad (2)$$

where  $d\epsilon: (1 - \epsilon_s)(1 - P_v)F\epsilon_v$ ,  $P_v: \left[ \frac{NDVI - NDVI_{min}}{NDVI_{max} - NDVI_{min}} \right]^2$ ,  $NDVI_{max}: 0.8$ , and  $NDVI_{min}: 0.1$ . A mean value of the shape factor  $F$  was assumed to be 0.55.

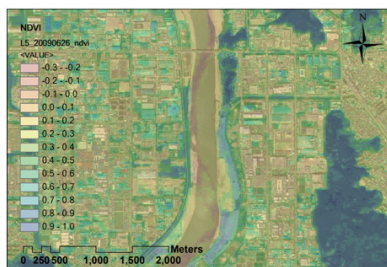
## 2.4 Land cover classification

The land cover types were classified into 50 classes using the unsupervised classification scheme by ISODATA and reduced to 5 classes by supervise classification using 5 bands from Band 1 through 5. The purpose of the classification was to check if NDVI values correspond to the actual land cover

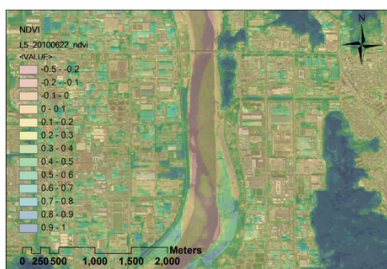
types. One of the difficulties in unsupervised classification might be segmenting vegetation, soil, and urban cover materials, which causes serious confusion in decision of each cover type for image pixels. Additional delineation for land cover types, especially for soil, was made by digitizing from aerial photos in 50 cm resolution.

### 3. NDVI characteristics of the urban covers

NDVIs for the study area in 2009 and 2010 was shown in Fig. 2a and b. The NDVI distribution of this area ranges from -0.21 to 0.94 and from -0.57 to 0.95 for 2009 and 2010 images, respectively. Most negative values were water or some urban land. Approximately  $\text{NDVI} \geq 0.45$  was mixed vegetation with other land covers like urban, soil, and/or water. In Fig. 2, vegetation was mapped correctly according to the vegetation density but some of the urban pixels, for example, factory rooftops, were unreasonably high in NDVI. The building rooftops of the upper left corners in Fig. 2(a) and (b) had distinguishable surface settings with a washboard pattern and blue color. These types of rooftops are presented in many places in Fig. 2 and seem to be a systematic phenomenon throughout the figure.



(a) NDVI image superimposed on aerial photo on June, 2009



(b) NDVI image superimposed on aerial photo on June, 2010

**Fig. 2. Characteristics of NDVI in the central Gumi area on (a) June, 2009 and (b) June, 2010**

To investigate more details on the surface settings vs. NDVI values, endmembers of five land cover types (i.e., factory roof, asphalt, soil, vegetation, and water) was segmented using digital topographic maps and manual digitizing and corresponding NDVI and LST values were extracted. In Fig. 3, each group of dots is considered to be a pure land cover material. Asphalt and rooftop were in fact very widely distributed and there were some case that NDVI values could be considered as full vegetation. Asphalt areas greater than 900 m<sup>2</sup> were difficult to be placed in the images and the areas often included line strips with white color. Therefore, the endmember pixels for asphalt were not actually pure and they were more distributed, which means that they cannot represent a typical NDVI value for asphalt. We found a typical NDVI value for soil was  $\cong 0.1$ . Full vegetation was found around the average  $\text{NDVI} = 0.79$  for both images. Water NDVIs were very different from other cover types and most negative values could be considered as water. Statistical summarization for NDVI and LST values was listed in Table 1 for the 2009 and 2010 images.

**Table 1. Statistics of NDVI and LST values for land covers**

		NDVI				Temperature			
		Ave.	Std.	Min.	Max.	Ave.	Std.	Min.	Max.
Roof	2009	0.23	0.14	-0.04	0.75	310.6	2.3	302.9	317.7
	2010	0.19	0.14	-0.06	0.77	309.6	2.1	302.9	317.7
Parking	2009	0.22	0.16	-0.03	0.89	309.6	2.8	298.7	315.8
	2010	0.21	0.17	-0.06	0.87	309.2	2.6	298.7	313.2
Soil	2009	0.12	0.02	0.00	0.41	309.3	1.9	304.1	312.4
	2010	0.10	0.02	-0.02	0.23	307.5	1.8	301.3	312.4
Water	2009	0.01	0.14	-0.22	0.70	301.0	2.3	297.9	315.5
	2010	-0.23	0.19	-0.56	0.72	299.1	1.8	296.6	312.4
Vegetation	2009	0.79	0.05	0.44	0.94	298.9	1.1	297.5	305.4
	2010	0.79	0.08	0.40	0.95	298.8	1.2	297.5	304.5

Interestingly, some of the rooftops in Fig. 3 are marked in the dense vegetation area. Using visual inspection, we found that there were systematic relationships of rooftop surface settings on NDVI values. For example, variations of color, brightness, and surface pattern and direction changed the NDVI values of rooftop regardless of vegetation. In other words, rooftops could have similarly high NDVI values

like vegetation. To investigate the details on the systematic relationships, the rooftop surfaces were characterized with color, illumination, and surface geometry like the number of washboard pattern.

The geometric pattern influence the color intensity. If the pattern can generate shadow resulting in dark colors, NDVI values were increased and LST decreased (Fig. 3). Note that LST decrease in shadowed areas might be correct in general (Bhang and Park, 2009).

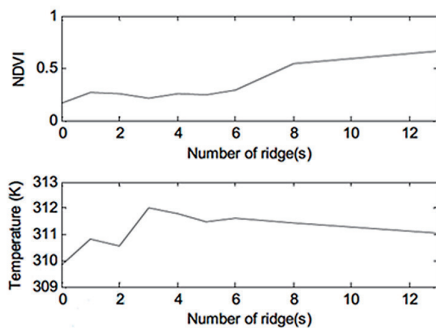


**Fig. 3. The influence of geometric pattern in building rooftop to NDVI and LST**

Fig. 4 shows the typical examples for high and low NDVI values of rooftops for the study area. The rooftop pixels in a circle at the upper left corner in Fig. 4 had NDVI = 0.75 and 0.77 for the 2009 and 2010 images, respectively, while the ones including white rooftop in the other circle were almost zero. The high NDVI rooftop had the washboard pattern with darker blue color relative to others. This washboard pattern more generated shadow resulting in darker color relative to other patterns (Fig. 4). Another case, the square at the bottom right, had the same rooftop pattern to the upper left circle but the reddish color was strikingly differentiated the NDVI value like 0.07. The two boxed cases with NDVI=0.15 and NDVI=0.56 at the middle left of Fig. 4 could not be effectively explained for the very different NDVI values. One of the possible explanation may be the direction of the washboard pattern, which means the higher one had a gully in the west-east direction that can be relatively easy to have shadow to the other case. By testing 47 building rooftops, we could have a possible conclusion that the dark (or shadowed) blue color usually had high NDVI values but other colors

like reddish or white fall into typical NDVI values for urban covers around 0 to 0.3. The surface pattern, in essence, contributed to generating shadow and seemed to influence NDVI values. These effects by color, shadow and surface pattern was briefly summarized in Table 3.

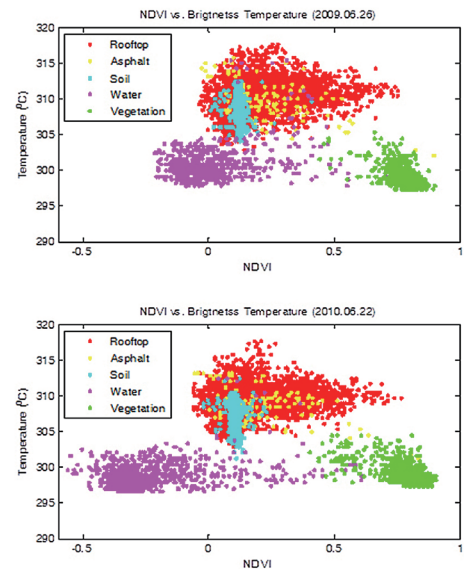


**Fig. 4. Distributions of normalized vegetation difference index (NDVI) and temperature for pixels of single-material classes. Note the relative distributions of the NDVI and temperature for each single material. The distribution does not consider the confidence interval to remove errors**



**Fig. 5. Factory roofs have various geometric patterns. The marked circles and squares indicates samples with highest to lowest normalized vegetation difference index (NDVI) values for the rooftops. The rooftop in the upper left circle is an example of the greatest NDVI value of 0.75 for the 2010 image. Temperatures and NDVIs roughly appear to have a positive relationship but not strictly**



**Table 2. The characteristics of NDVIs for building roofs**

	Min. NDVI		Max. NDVI
Range	-0.06	↔	0.78
Color	Reddish brown, orange, white		Blue
Shadow	Bright		Dark
Geometry	Flat		Complex (Washboard)

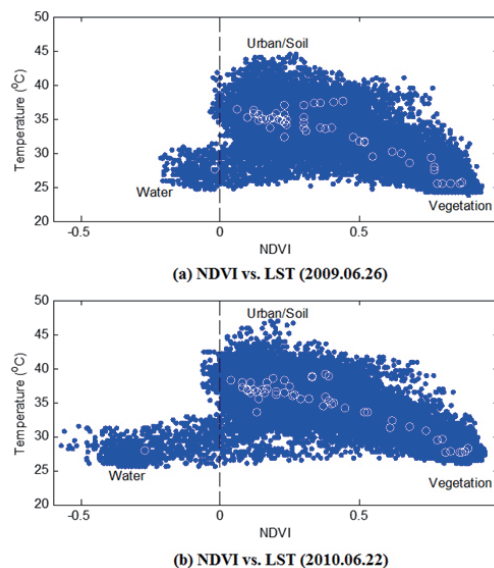
#### 4. Transition of NDVI by Mixing

Fig. 5 shows that NDVIs in urban areas are basically mixtures of three different land cover groups, soil/urban, water, and vegetation. Interestingly, all urban land cover types could be basically separated based on two groups of materials, vegetation and soil/urban covers if we separate water since it has a very different spectral characteristics. As found in many articles, most of the NDVIs in Fig. 5 were negatively distributed between two major components of soil/urban and vegetation depending on a mixture condition of vegetation. The average values of NDVI and temperature for each class clearly illustrated the negative relationship appear to be linear. However, they are not a general fact since other studies showed non-linear negative relationship. Water has a very different physical property from soil/urban covers so that the distribution could be explained to have a weak positive relationship of NDVI with temperature.

Using Fig. 6, three transitions depending on the mixture of the three land cover types can be assumed.

(1) *Vegetation vs. urban/soil transition*: Most pixels were distributed between urban/soil and vegetation, suggesting that the mixture of urban/soil and vegetation was the most frequent mixture combination in the urban area. The wide distribution around the urban/soil center rather than that of vegetation may have been due to the two pathways; one between urban and vegetation (the right edge of the yellow triangle in Fig. 6(a)) and the other between soil and vegetation (the right edge of the dark gray triangle in Fig. 6(b)) so that in the urbanization process, vegetation cover changed to urban or bare soil. The transition of vegetation to urban decreased the NDVI values with a faster increase in surface temperature. For the vegetation to soil, NDVI decreased with the transition

to urban but the surface temperature increased relatively slowly for the transition to urban. These facts indicate that the variations of transitions of soil and urban covers can be changed radically depending on the materials even though the NDVI values have the same range of the materials so it is difficult to distinguish the urban covers with NDVI values.

**Fig. 6. Distribution of LSTs for NDVIs**

(2) *Urban/soil vs. water transition*: Water may hardly be mixed in the urban area relative to soil so the distribution density between the urban and water distribution centers in Fig. 6 was sparse along the dark blue edge between urban and water. In contrast, water might be more frequently mixed with soil rather than urban; thus, more pixels could be observed between soil and water along the yellow edge of the triangle. Note that mixing of urban vs. water did not occur in the study area.

(3) *Water vs. vegetation transition*: The mixture of water and vegetation may not be frequent but possibly occur because shallow water with green vegetation can be found at shores of rivers, streams, lakes, or wetlands as was true in the study area. Additionally, the water content in vegetation may be included. However, the relationship between NDVI and temperature was opposite to the general case between urban/soil vs. vegetation, indicating a positive relationship. The reasons may be due to the thermal properties of water such

as high specific heat capacity. Water needs a large amount of energy to raise its temperature but the sediments in water may contribute to heating it. Sediments can be various forms of materials and we suspected that the small soil and vegetation cover might affect the transition of water toward soil and vegetation.

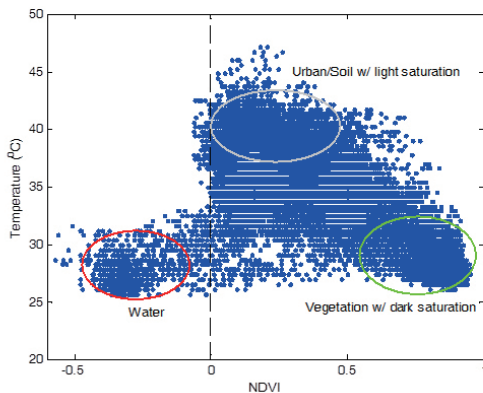


**Fig. 7. Normalized vegetation difference index (NDVI) and temperature values for the all image pixels in the study area. Urban/soil, vegetation, and water are circled and their relationship with NDVI and temperature appeared to follow the lines of the yellow and dark-blue triangles by the mixture of the three materials**

## 5. Conclusion

The urban NDVI values in remote sensing images are affected by the mixture of various land cover materials. Asphalt had essentially the same NDVI distributions as surface temperature on rooftops, and the covers could be grouped into the urban category. Soil could be the different statistical characteristics but they were in the wide ranges of NDVI and temperature distributions in the urban. It was difficult to distinguish urban from soil in practice. The most important finding in this study is that NDVI values may be problematic when urban covers are portrayed with the NDVI; for example, the building rooftop with different colors and geometric shapes influence the NDVI values. This may cause incorrect NDVI values so that high NDVI values come with blue and complex geometric surface patterns generating shadow. These incorrect NDVI values might eventually result in incorrect LSTs especially in urban areas if NDVI is

used for the emissivity calculation by Sobrino *et al.* (2004). In conclusion, users using NDVI should be very careful in applications to urban areas.

Our investigation also indicated that the three types of transitions of land covers could be defined in terms of NDVI; urban/soil, vegetation and water by considering the NDVI characteristics of urban and soil. Based on the categories, three transition scenarios could be described that depended on the dominance of urban and soil, as the mixture with vegetation followed a slightly different pathway. Similarly, the mixture with water also appeared to follow two pathways. Finally, the NDVI and temperature between water, usually excluded in other studies for the urbanization process, and other categories had a positive relationship unlike between urban/soil and vegetation.

## Acknowledgment

This paper was supported by Research Fund, Kumoh National Institute of Technology.

## References

- Bhang, K.J. and Park, S.S. (2009), Evaluation of the surface temperature variation with surface settings on the urban heat island in Seoul, Korea, using Landsat-7 ETM+ and SPOT, *IEEE Geoscience and Remote Sensing Letters*, Vol. 6, no. 4, 708-712.
- Carlson, T.N., Gillies, R.R., and Perry, E.M., (1994), A method to make use of thermal infrared temperature and NDVI measurements to infer surface soil water content and fractional vegetation cover. *Remote Sensing Reviews*, Vol. 9, pp. 161-173.
- Gillies, R.R. and Carlson, T.N. (1995), Thermal remote sensing of surface soil water content with partial vegetation cover for incorporation into climate models. *Journal of Applied Meteorology*, Vol. 34, pp. 745-756.
- Gallo, K.P., McNab, A.L., Karl, T.P., Brown, J.F., Hood, J.J., and Tarpley, J.D. (1993), The use of a vegetation index for assessment of the urban heat island effect, *International Journal of Remote Sensing*, Vol. 14, pp. 2223-2230.
- Gallo, K.P., Tarpley, J.D., McNab, A.L., and Karl, T.R. (1995),

- Assessment of urban heat islands: a satellite perspective, *Atmospheric Research*, Vol. 37, pp. 37-43.
- Jiménez-Muñoz, J.C., Cristobal, J., Sobrino, J.A., Soria, G., Ninyerola, M., Pons, X., and Pons, X. (2004), Revision of the single-channel algorithm for land surface temperature retrieval from Landsat thermal-infrared data, *IEEE Transactions on Geoscience and Remote Sensing*, Vol. 47, pp. 339-349.
- Owen, T.W., Carlson, T.N., and Gillies, R.R. (1998), An assessment of satellite remotely-sensed land cover parameters in quantitatively describing the climatic effect of urbanization, *International Journal of Remote Sensing*, Vol. 19, pp. 1663-1681.
- Price, J.C. (1990), Using spatial context in satellite data to infer regional scale evapotranspiration, *IEEE Transactions on Geosciences and Remote Sensing*, Vol. 28, pp. 940-948.
- Sobrino, J.A., Jiménez-Muñoz, J.C., and Paolini, L. (2004), Land surface temperature retrieval from LANDSAT TM 5, *Remote Sensing of Environment*, Vol. 90, pp. 434-440.
- Southworth, J. (2004), An assessment of Landsat TM band 6 thermal data for analysing land cover in tropical dry forest regions, *International Journal of Remote Sensing*, Vol. 25, pp. 689-706.
- Stagakis, S., Markos, N., Sykioti, O., and Kyparissis, A. (2010), Monitoring canopy biophysical and biochemical parameters in ecosystem scale using satellite hyperspectral imagery: an application on a *Phlomis fruticosa* Mediterranean ecosystem using multiangular CHRIS/PROBA observations. *Remote Sensing of Environment*. Vol. 114, pp. 977-994.
- Valor, E. and Caselles, V. (1996), Mapping land surface emissivity from NDVI: application to European, African and South American areas. *Remote Sensing of Environment*, Vol. 57, 167 – 184.
- Weeks, J.R. (2010), *Remote Sensing of Urban and Suburban Areas, Remote Sensing and Digital Image Processing*, Springer, New York.
- Wu, C. and Murray, A.T. (2003), Estimating impervious surface distribution by spectral mixture analysis, *Remote Sensing of Environment*, Vol. 84, pp. 493-505.
- Yue, W., Xu, Y., Tan, W., and Xu, L. (2007), The relationship between land surface temperature and NDVI with remote sensing: application to Shanghai Landsat 7 ETM+ data, *International Journal of Remote Sensing*, Vol. 28, pp. 3205-3226.
- Yuan, F. and Bauer, M.E. (2007), Comparison of impervious surface area and normalized difference vegetation index as indicators of surface urban heat island effects in Landsat imagery, *Remote Sensing of Environment*, Vol. 106, pp. 375-386.